Capsular flow in pipelines

By A. E. VARDY

Department of Civil Engineering, University of Leeds

M. I. G. BLOOR

Department of Applied Mathematics, University of Leeds

AND J. A. FOX

Department of Civil Engineering, University of Leeds

The problem considered is that of the steady motion of a series of neutrally buoyant, flat-faced, rigid, cylindrical capsules along the axis of a pipeline under the influence of a hydraulic pressure gradient. The Navier–Stokes equations are non-dimensionalized and expressed in central-difference form. Numerical solutions are found by the method of relaxation for Reynolds numbers up to 20 000 and a close agreement is obtained with readings from a laboratory apparatus for Reynolds numbers up to 2200.

The flow is examined in detail and the existence of toroidal vortices between successive capsules is demonstrated. Their shape is shown to be increasingly influenced by inertial forces as the Reynolds number increases, but the overall pressure gradient is not greatly dependent on the Reynolds number.

1. Introduction

In recent years, considerable interest has been shown in the flow of capsules along pipelines. Several common applications exist, ranging from transportation systems to capillary blood flow. The latter case has been found to be particularly well suited to mathematical analysis because capillaries are very small and creeping-flow solutions are sufficient.

Bloor (1968) approximated blood corpuscles by a series of flat-faced rigid cylindrical capsules flowing axially along a pipeline. He solved the linearized Navier–Stokes equations numerically and investigated the effect of varying the size and spacing of the capsules on the overall pressure gradient. Lew & Fung (1969) and Bugliarello & Hsiao (1970) considered a similar model and dealt with the streamline pattern in the interspaces between successive capsules. Wang & Skalak (1969) treated the corpuscles as a line of spherical capsules, and Chen & Skalak (1970) dealt with both oblate and prolate spheroids. These are more analogous to the true biconcave shape of the red blood corpuscles. Brenner (1970) extended the scope of the analysis to the unsymmetrical case of eccentrically positioned, neutrally buoyant spheres. Experimental evidence was obtained by Hochmuch & Sutera (1970) to verify a theoretical prediction that a line of spherical

caps is stable on the axis of a pipeline if the curved surfaces are facing down-stream. More recently, Duda & Vrentras (1971 a, b) have derived a new analytical solution to the creeping-flow problem. They have also extended the solution to include heat-transfer terms to represent the chemical transfers which take place through the capillary walls. These papers all deal with fairly close-fitting capsules and are complementary to a study by Lighthill (1968), who considered the special case of a large distensible corpuscle passing through a distensible capillary of a nominally smaller diameter. By using lubrication theory, he predicted a build-up of pressure at the capillary wall just in front of the corpuscles, thus explaining the experimentally observed shape of capillaries as large corpuscles pass along them.

Higher Reynolds number flows have been less extensively considered, but Charles (1963) presented a simplified analysis of the motion of single capsules in a pipeline with the fluid in laminar or turbulent flow. Kennedy (1966) suggested a modification to Charles's turbulent-flow analysis, and Newton, Redberger & Round (1964) presented a more rigorous solution for the laminar-flow case. They used a linearized form of the Navier–Stokes equations to obtain a series of numerical solutions corresponding to various capsule sizes, shapes and eccentricities.

There is a similar problem in two dimensions when flow passes over a corrugated duct, and various attempts have been made to analyse it. The creeping-flow case was studied by Weiss & Florsheim (1965), who presented an analytical solution and verified experimentally that it was reasonably valid for Reynolds numbers below 150. They also predicted and demonstrated the existence of higher order vortices in deep narrow cavities. Similar vortices in the corners of rectangular cavities had previously been predicted by Rayleigh (1920) and subsequently by Moffatt (1964). Burggraf (1966) and Bye (1966) simultaneously derived solutions for Reynolds numbers up to 700, but both found that the results of the numerical analysis oscillated strongly when the Reynolds number exceeded 400. Runchal & Wolfshtein (1969) attributed this phenomenon to the use of central-difference formulae. They demonstrated that solutions can be obtained for Reynolds numbers as high as 10000 if end-difference formulae are applied. They used a very coarse mesh size and did not suggest that their results would be physically meaningful. However, they predicted that meaningful solutions would be obtainable by their method if a sufficiently small mesh size was used.

In this paper, a series of flat-faced rigid cylindrical capsules is considered as it moves at a steady speed along the axis of a pipeline under the influence of a hydraulic pressure gradient. The capsules are neutrally buoyant and regularly spaced and are very long in comparison with the width of the annuli between them and the pipeline. A numerical solution of the Navier–Stokes equations is presented and central-difference formulae are used because the fundamental equation does not suffer from the limitation which caused Runchal & Wolfshtein to recommend end-difference approximations. Solutions are readily obtained for Reynolds numbers up to 2000, and consistent answers are produced even at Reynolds numbers as high as 5000. The existence of a large toroidal vortex in the interspace between successive capsules is demonstrated at all Reynolds numbers.

It is usual to expect pipeline laminar flow to become unstable soon after the Reynolds number exceeds 2000, but it is possible that, in practice, the presence of capsules will help to stabilize laminar flow at higher Reynolds numbers. The flow in the annuli will remain laminar until much higher Reynolds numbers because the flow width is much less than the pipe radius. If the capsules remain stably positioned on the pipeline axis, the flow in the interspaces between them might also remain laminar. The annuli would then be analogous to the entry and exit regions in laboratory pipelines in which Poiseuille flow can be retained for Reynolds numbers as high as 50000.

Although very unlikely, the laminar capsular flow mechanism, if stable at high Reynolds numbers, could prove to be a more efficient method of fluid transport than high Reynolds number turbulent flow without capsules present. The feasibility of this would depend upon the length of capsules required to provide a sufficiently stable boundary condition for the interspace flow.

2. Basic equations

A system of cylindrical polar co-ordinates, moving with the capsules, is chosen so that the tube wall moves with a velocity U in the direction of its axis. The flow is steady and two-dimensional relative to these axes and the radial and axial distances from the centre of a capsule are denoted by r and z respectively (see figure 1).

The Navier–Stokes equations become

$$v\frac{\partial v}{\partial r}+u\frac{\partial v}{\partial z} = -\frac{1}{\rho}\frac{\partial p}{\partial r}+\nu\left[\frac{\partial^2}{\partial r^2}+\frac{1}{r}\frac{\partial}{\partial r}+\frac{\partial^2}{\partial z^2}-\frac{1}{r^2}\right]v, \tag{1}$$

and

$$v\frac{\partial u}{\partial r}+u\frac{\partial u}{\partial z} = -\frac{1}{\rho}\frac{\partial p}{\partial z}+\nu\left[\frac{\partial^2}{\partial r^2}+\frac{1}{r}\frac{\partial}{\partial r}+\frac{\partial^2}{\partial z^2}\right]u, \tag{2}$$

and the continuity equation is $v/r+\partial v/\partial r+\partial u/\partial z = 0$. A stream function Ψ defined by

$$u = \frac{1}{r}\frac{\partial\Psi}{\partial r}, \quad v = -\frac{1}{r}\frac{\partial\Psi}{\partial z} \tag{3}$$

is introduced to satisfy the continuity equation.

The flow variables are non-dimensionalized so that, denoting non-dimensional quantities by a prime,

$$u' = u/U, \quad v' = v/U, \quad p' = p/\rho U^2,$$

$$r' = r/R, \quad z' = z/R, \quad \Psi' = \Psi/UR^2,$$

where U is the velocity of the tube relative to the axes, R is the radius of the tube and ρ is the density of the liquid. For convenience, the primes are omitted in the remainder of the text. No confusion will result if all variables are assumed to be non-dimensional unless otherwise specified.
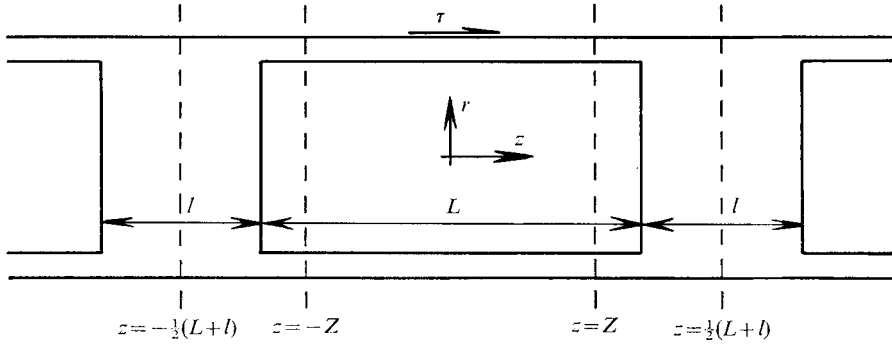
FIGURE 1. Notation for the capsule geometry.

After elimination of the pressure terms from (1) and (2) and substitution of the expressions specified in (3) for u and v, the equation for Ψ becomes

$$\frac{Re}{2}\left[\frac{\partial\Psi}{\partial z}\left\{-\frac{1}{r}\frac{\partial^3\Psi}{\partial r^3}+\frac{3}{r^2}\frac{\partial^2\Psi}{\partial r^2}-\frac{3}{r^3}\frac{\partial\Psi}{\partial r}-\frac{1}{r}\frac{\partial^3\Psi}{\partial r\partial z^2}+\frac{2}{r^2}\frac{\partial^2\Psi}{\partial z^2}\right\}\right.$$
$$\left.+\frac{\partial\Psi}{\partial r}\left\{\frac{1}{r}\frac{\partial^3\Psi}{\partial r^2\partial z}-\frac{1}{r^2}\frac{\partial^2\Psi}{\partial r\partial z}+\frac{1}{r}\frac{\partial^3\Psi}{\partial z^3}\right\}\right]=\left[\frac{\partial^2}{\partial r^2}-\frac{1}{r}\frac{\partial}{\partial r}+\frac{\partial^2}{\partial z^2}\right]^2\Psi, \quad (4)$$

where Re is a Reynolds number, defined by $Re = 2UR/\nu$. The pressure distribution can be determined from (1) and (2).

Equation (4) is solved within the region between the centre planes of successive capsules. It must therefore satisfy the following boundary conditions. On the tube wall, where $r = 1$, Ψ = constant and $\partial\Psi/\partial r = 1$; on the capsule surfaces, $\Psi = \partial\Psi/\partial r = \partial\Psi/\partial z = 0$; on the central axis, $\Psi = 0$ and by symmetry, $\partial\Psi/\partial r = 0$. The capsules are sufficiently long for the flow in the annuli between them and the tube wall to be independent of z except near the capsule faces. In these annular regions, say where $|z| < Z$, the flow is therefore described by

$$\Psi = Re\,P_g\frac{(r^2-a^2)^2}{32}+\frac{[r^2-a^2-2r^2\ln{(r/a)}]}{4\ln{(a)}}\left[1-Re\,P_g\frac{1-a^2}{8}\right], \quad (5)$$

where P_g is a constant denoting the local value of $\partial p/\partial z$, and a is the radius of a capsule. P_g is an unknown which is found by considering the equilibrium of the fluid.

In figure 1, τ denotes the shear stress exerted by the wall on the fluid in the positive z direction. The equation of equilibrium of the fluid in the region between the centre planes of successive interspaces may be written as

$$\pi\{p[1,\tfrac{1}{2}(L+l)]-p[1,-\tfrac{1}{2}(L+l)]\} = 2\pi\int_{-\frac{1}{2}(L+l)}^{\frac{1}{2}(L+l)}\tau(z)\,dz, \quad (6)$$

where L and l denote the lengths of a capsule and an interspace respectively. In deriving (6), account has been taken of the fact that the capsule imposes no net force on the fluid. Also, the flows at $z = \pm\frac{1}{2}(L+l)$ are identical and so the value of $p[r,\frac{1}{2}(L+l)]-p[r,-\frac{1}{2}(L+l)]$ is independent of r. The pressure forces are therefore simply given by the left-hand side of (6), with $r = 1$ being chosen for convenience.
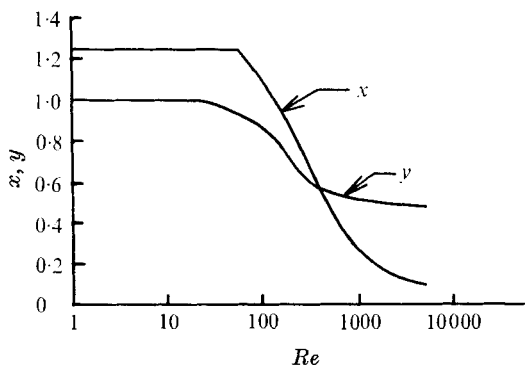
FIGURE 2. Typical values of the relaxing factor x and the initial-value multiplier y used to generate solutions at high Reynolds numbers from known solutions at lower Reynolds numbers. $a = 0.90$, $l = 1$ and $h = \frac{1}{10}$.

The fall in pressure at the wall between the two centre planes can be expressed as the sum of the fall in the region $|z| < Z$ (i.e. $2Z P_g$) and the falls in the regions $Z < |z| < \frac{1}{2}(L+l)$. In the latter regions, the pressure fall and also $\tau(z)$ are evaluated from the numerical solution, so that, within $|z| < Z$, where $\tau(z)$ is a constant given by $(2/Re)\,[\partial u/\partial r]_{r=1}$, the pressure gradient satisfying the equation of equilibrium (6) is

$$P_g = \frac{1}{1-a^2}\left[\frac{8}{Re} + N\ln(a)\right],\tag{7}$$

where

$$N = \frac{1}{Z}\left[\int_{-\frac{1}{2}(L+l)}^{-Z}\left\{\frac{\partial p}{\partial z}\bigg|_{r=1} - 2\tau(z)\right\}dz + \int_Z^{\frac{1}{2}(L+l)}\left\{\frac{\partial p}{\partial z}\bigg|_{r=1} - 2\tau(z)\right\}dz\right].\tag{8}$$

3. Numerical solution

Equation (4) is expressed in central-difference form and is solved by the method of relaxation, using a KDF 9 computer. As a first guess, Ψ is chosen to be zero at each mesh point in a regular rectangular mesh occupying the region under consideration, and the boundary conditions are included in the usual way. However, those boundary conditions which are governed by (5) specify Ψ as a function of P_g and a. Since P_g is unknown, its value is found by an iterative method superimposed on the relaxation scheme. Initially the value of N is guessed to be zero so that $P_g = 8/Re(1-a^2)$ and $\Psi = (r^2-a^2)^2/4(1-a^2)$, values corresponding to the case of an infinitely long capsule. More accurate values for N are derived from successive solutions for Ψ by using (8), so that (4) and (5) are solved simultaneously. In practice, it is more convenient to retain the initially chosen value for Ψ on the tube wall and to allow a to vary to satisfy (5) when subsequent values are obtained for N. Only very small changes in the geometry are caused by this technique.

A better initial approximation for the Ψ distribution throughout the region at any Reynolds number can be derived from a known solution at a different Reynolds number by multiplying each element of the known solution by a constant y.
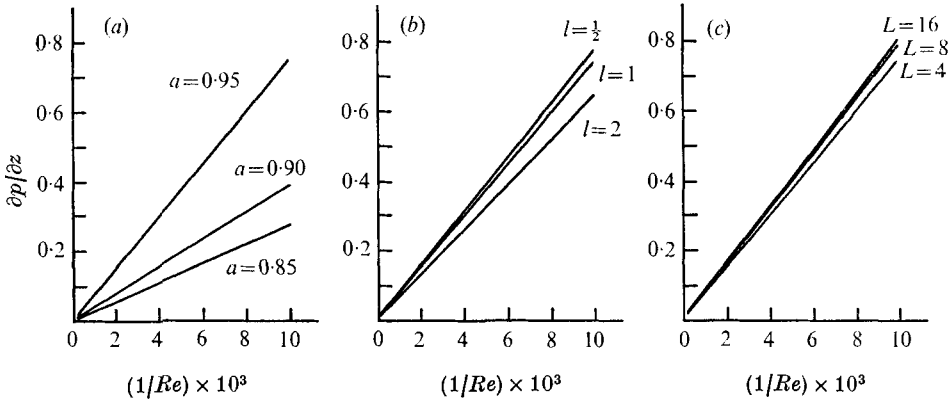
FIGURE 3. The influence of the geometry on the relationship between the overall pressure gradient $\partial p/\partial z$ and the Reynolds number. (a) $l = 1$, $L = 4$. (b) $L = 4$, $a = 0.95$. (c) $l = 1$, $a = 0.95$.
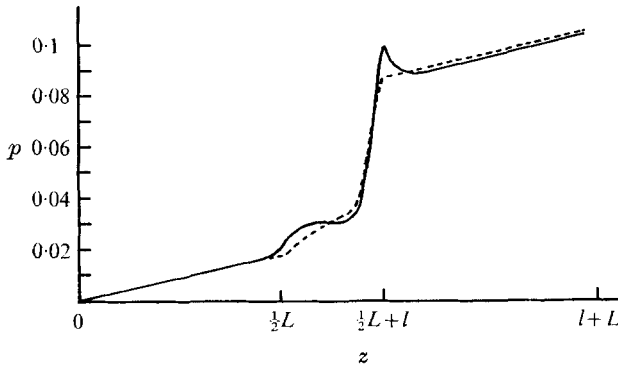
FIGURE 4. A typical pressure distribution along the tube wall. At the coarser mesh size, the shape is less well predicted, but the total pressure drop varies only slightly. $a = 0.90$, $l = 1$, $L = 4$ and $Re = 2000$. $---$, $h = \frac{1}{10}$; $—$, $h = \frac{1}{40}$.

Some typical values of this constant, which would produce good initial guesses for solutions at double the Reynolds number of various known solutions, are shown in figure 2. They are found only by trial and error, and depend strongly upon the geometry and the mesh size used.

A series of solutions corresponding to nominal capsule radii of 0.85, 0.90 and 0.95, capsule lengths of 2, 4, 8, 16 and 10^6, interspace lengths of $\frac{1}{2}$, 1 and 2, and Reynolds numbers from 1 to 5000 has been derived using mesh sizes of $h = \frac{1}{10}$, $\frac{1}{20}$, $\frac{1}{40}$ and $\frac{1}{80}$. It has been found to be advantageous to over-relax when the Reynolds number is low, but essential to under-relax at high Reynolds numbers, when the linear terms no longer dominate in equation (4). An indication of the degree of under-relaxing required to prevent divergence is shown in figure 2, in which x is the largest relaxing factor which will permit convergence.
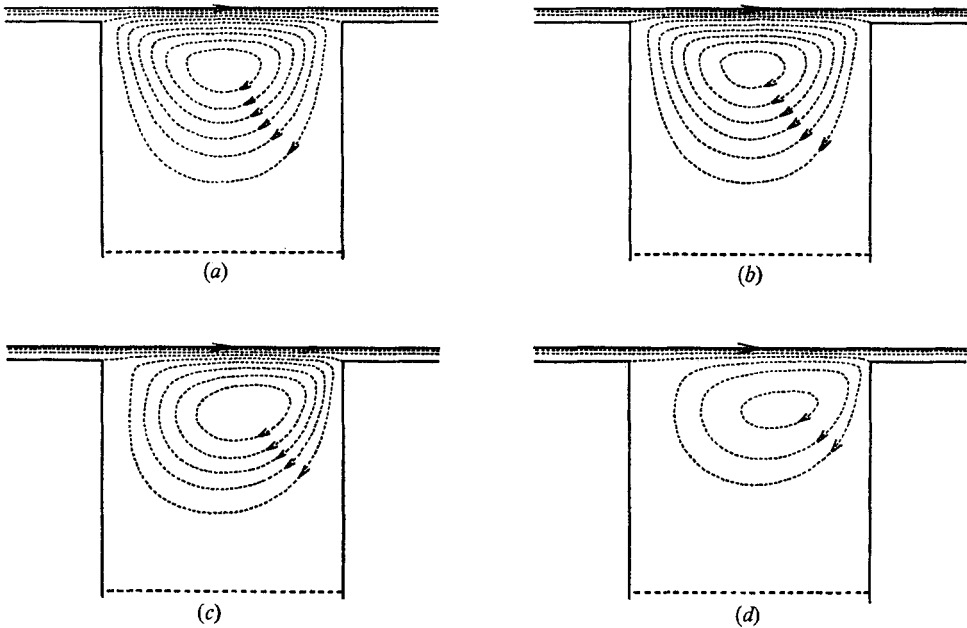
FIGURE 5. Typical interspace streamline patterns; $a = 0.95$, $l = 1$, $L = 4$.
(a) $Re = 1$. (b) $Re = 100$. (c) $Re = 500$. (d) $Re = 2000$.

4. Results

A nearly linear relationship has been found between the tube velocity and the overall axial pressure gradient required to hold the capsules in position. In practice, this is the pressure gradient required to force the capsules along the pipeline at a steady velocity. Its value increases with the length and diameter of the capsules, but decreases as the length of the interspaces increases (see figure 3).

The consistency of the solutions has been found to be extremely good when the smaller mesh sizes are used. For Reynolds numbers below 2000, the maximum recorded difference between the overall pressure gradients predicted with mesh sizes of $\frac{1}{40}$ and $\frac{1}{80}$ is just less than 0.2 %. With a mesh size of $\frac{1}{10}$, the difference is greater, but there is still less than a 3 % variation between it and the corresponding solution with a mesh size of $\frac{1}{80}$ when the Reynolds number reaches 5000. Nevertheless, the local axial pressure distribution along the tube wall is not predicted accurately when coarse mesh sizes are used because insufficient information is obtained about the flow near the ends of the annuli. Figure 4 shows the distribution predicted with mesh sizes of $\frac{1}{10}$ and $\frac{1}{40}$ for a typical set of values for a, l, L and Re. With the mesh size of $\frac{1}{10}$, equation (5) is assumed to apply right up to the ends of the annuli. The two curves differ considerably, but the approximate solution would be quite satisfactory for almost any practical circumstance.

Considerably less computing store and time is, of course, required for calculations using coarser mesh sizes. For example, about 10 min of run time and less than 100 words of data store are required to compute a solution for a Reynolds number of 2000 from a known solution at a Reynolds number of 1000 if a mesh size

of $\frac{1}{10}$ is used. A comparable solution using a mesh size of $\frac{1}{80}$ would typically require almost 50 min of run time and over 6000 words of data store.

Since the overall axial pressure gradient is closely predicted even when the flow at the ends of the annuli is poorly described, it is deduced that the flow in an interspace is not strongly dependent upon the velocity distribution in the annuli. In particular, it is nearly independent of the length of the capsules, a property which leads to great savings in computing time. This independence of the interspace flow is explained by the streamline patterns such as those drawn relative to the capsules in figure 5. At all Reynolds numbers, a $\Psi = 0$ streamline separates the annulus flow from the interspace vortex and there is thus no interchange of fluid between the two regions. Next to the tube wall, the flow generating the vortex is far less restrained than it is in the annuli and so is not greatly influenced by the conditions in the annuli. In particular, it is very insensitive to small changes in the velocity profile at the ends of the annuli resulting from changes in the pressure gradient.

At low Reynolds numbers, viscous forces dominate the flow and the streamline pattern is almost symmetrical. As the Reynolds number increases, however, inertia forces destroy the symmetry and shift the vortex centre towards the trailing capsule. This effect resembles that in the two-dimensional case discussed by Burggraf (1966) except that there is no evidence of a shift back towards the centre of the interspace at higher Reynolds numbers.

Figures 4 and 5 refer to capsules of different diameters, but they may be compared because the pressure distribution curve displays the same features for both cases. It is clear from (2) that, at the tube wall, the axial pressure gradient balances the skin friction and the radial rate of change of the skin friction. Well inside an annulus, these values are almost independent of z and so the pressure gradient is nearly constant. However, when the fluid enters an interspace, it is less restrained near the wall and the pressure gradient temporarily increases to balance the rapid rate of change of the skin friction. A similar but larger increase in the pressure gradient occurs just in front of the leading face of each capsule, where inertial forces cause a much more rapid rate of change in the skin friction. The pressure at the wall reduces just inside the next annulus, where the radial velocity distribution adjusts to accommodate the restriction imposed by the capsule side. As a consequence of the pressure rise just in front of the capsules, the pressure gradient in the annuli reverses at high Reynolds numbers so that the state of equilibrium described by (6) is maintained (see figure 7).

Figure 5 shows the streamline $\Psi = 0$ joining the corners of successive capsules over the entire range of Reynolds numbers. Since the stream function is evaluated only at the mesh points, this indicates only that the $\Psi = 0$ streamline meets the capsules within one mesh length of the corners. Nevertheless, a fourth-order interpolation scheme is used when plotting the streamlines and so the positioning of the line within this grid length should be fairly accurate. Further $\Psi = 0$ streamlines indicating the existence of higher order vortices might be expected nearer the tube axis when the capsules are closer together (see Bloor 1968), but these geometries have not been considered in the present study. Very weak secondary vortices analogous to those described by Moffatt (1964) for the two-dimensional case are found near the centre of the capsules' leading faces at high

Reynolds numbers. However, they have been ignored because they are of little practical interest and their shape and size is greatly dependent on small numerical fluctuations in the iterative procedure used.

It has been suggested in the introduction that laminar flow might remain stable at high Reynolds numbers when capsules are present. A series of results for $a = 0.95$, $l = 1$ and $L = 4$ has therefore been derived for Reynolds numbers up to 20000, using a mesh size of $\frac{1}{80}$. This is too coarse to give accuracy, but it must be noted that the overall pressure gradient has been predicted to within 3 % at all Reynolds numbers below 5000 when using a far coarser mesh size ($\frac{1}{10}$). It is therefore considered likely that the overall pressure gradient will have been reasonably well predicted at a Reynolds number of 20000 when using the mesh size $h = \frac{1}{80}$. Indeed, the oscillations in the solution do not cause this overall value to vary by more than about 1 %. Nevertheless, the point at which laminar flow will break down can be determined only experimentally. The numerical results have therefore been compared with experimental readings obtained from a laboratory apparatus.

5. Experiments and discussion

The apparatus consists of a 12 m length of 50 mm bore tubing joining two large storage tanks, one of which is 1 m higher than the other. With the system filled with oil, the rate at which oil flows under gravity through the pipeline into the lower tank is governed by the degree of closure of a valve beneath the upper tank. A series of pressure transducers, mounted along the pipeline, is used to study the pressure history as a line of 47·5 mm diameter capsules passes along a 4 m section of very close tolerance bore tubing in the centre of the pipeline. The transducers are described in detail by Vardy (1971) and are developed from similar instruments described by Fox & Henson (1969). A photo-electric cell is used to measure the percentage of a light beam passing between a fixed plate and a moving diaphragm which is hydraulically connected to the fluid in the pipeline. The cell is electrically connected as one arm of a Wheatstone bridge circuit which powers an ultraviolet light recorder without amplification.

Successive capsules are joined by a thin nylon thread which is trapped into flush-fitting plugs screwed into the centres of the capsule faces. The thread passes through a piece of 1·25 mm o.d. brass tubing, the length of which determines the spacing between the capsules. These connexions prevent axial displacement of the capsules relative to one another, but impose no other restraint on their motion. The capsules are very nearly neutrally buoyant in the oil, and eight small steel balls mounted in their walls ensure that they remain symmetrically positioned on the axis of the pipeline. Onset of the 'stick and slip' mechanism is therefore prevented.

Readings have been obtained for a series of capsule spacings and velocities. The overall pressure gradient is in general about 5 % greater than the predicted value at Reynolds numbers up to 2200 (figures 6, 7). This indicates a better agreement between theory and practice than is at first apparent because observations made during the experimental tests indicated that the measured
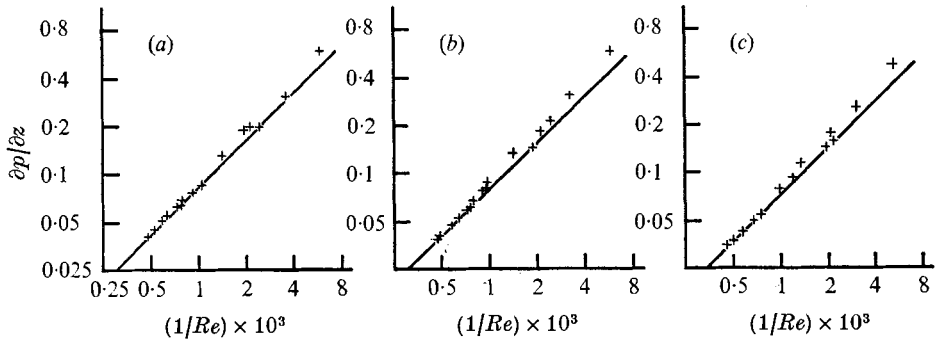
FIGURE 6. Overall pressure gradients: +, experimental results; —, theoretical (solid line) results. $L = 4$, $a = 0.95$. (a) $l = \frac{1}{2}$. (b) $l = 1$. (c) $l = 2$.
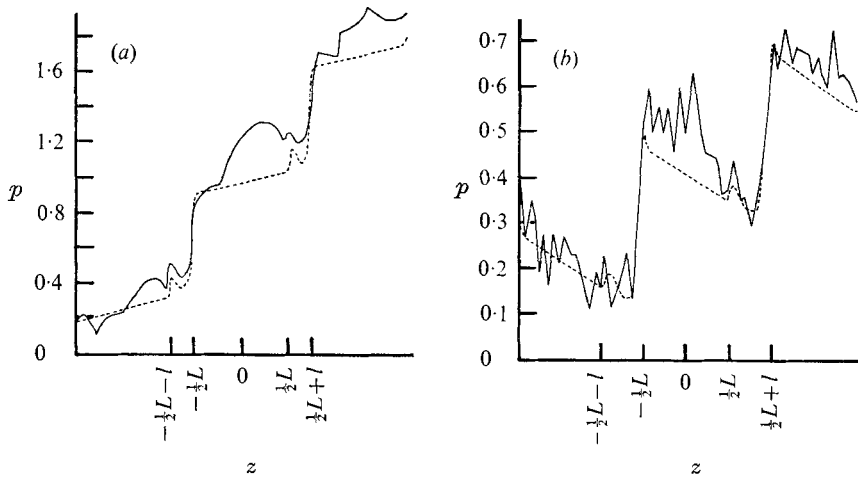
FIGURE 7. Typical measured (solid line) and predicted (broken line) pressure distributions along the tube wall. (a) $l = 1$, $Re = 520$. (b) $l = 2$, $Re = 2196$.

pressure gradient would exceed the theoretically predicted value. The motion of the capsules was clearly audible at all speeds, and so the steel balls must have been scraping along the pipeline wall. This also explains the tendency for the errors to be greatest at lower speeds, when the capsules would be touching the pipeline more often.

With the theoretical curve of figure 7 (a) 'stretched' to allow for this effect, the measured pressure line in each annulus crosses the predicted curve. This effect has been found to occur when the capsules are not quite parallel to the axis of the tube because of small variations in the projections of the steel balls above the surfaces. Also, strong nonlinearities in the pressure distribution exist locally around the balls, where the flow pattern is disturbed. For example, the sharp 'valley' near the origin of the figure coincides exactly with the spacing of the balls along the capsules. Figure 7 (b) shows a close agreement with the predicted curve, but many peaks exist on the pressure traces. These are largely a result of the capsules hitting the sides of the tube, especially at one of the many places where

the tube is scratched along its circumference. The apparatus is otherwise relatively free from disturbances.

In an attempt to investigate the stability of the mechanism at higher Reynolds numbers, further readings have been taken using a less viscous oil. Unfortunately, no rigorous conclusions can be drawn because the pipeline is too short to allow the capsules to reach a steady speed. However, a visual inspection of the flow in a transparent section of the pipeline indicates that the flow is still everywhere laminar. Reynolds numbers of over 7000 have been reached, and yet dust particles in the oil appear to follow closed streamlines in the interspaces. No evidence of a transfer of fluid between the interspaces and the annuli can be found. It is unfortunate that no more rigorous results for high Reynolds number operation are available, but the work has been undertaken as a part of a postgraduate study and it has not been feasible to re-design the apparatus to cover the high Reynolds number range.

REFERENCES

BLOOR, M. I. G. 1968 *Phys. Med. Biol.* **13**, 443.

BRENNER, H. 1970 *J. Fluid Mech.* **43**, 641.

BUGLIARELLO, G. & HSIAO, G. C. 1970 *Biorheology*, **7**, 5.

BURGGRAF, O. R. 1966 *J. Fluid Mech.* **24**, 113.

BYE, J. A. T. 1966 *J. Fluid Mech.* **26**, 577.

CHARLES, M. E. 1963 *Can. J. Chem. Eng.* **41**, 46.

CHEN, T. C. & SKALAK, R. 1970 *Appl. Sci. Res.* **22**, 403.

DUDA, J. L. & VRENTRAS, J. S. 1971a *J. Fluid Mech.* **45**, 247.

DUDA, J. L. & VRENTRAS, J. S. 1971b *J. Fluid Mech.* **45**, 261.

FOX, J. A. & HENSON, D. A. 1969 *The Engineer,* **229**, 53.

HOCHMUCH, R. M. & SUTERA, S. P. 1970 *Chem. Eng. Sci.* **25**, 593.

KENNEDY, R. J. 1966 *Can. J. Chem. Eng.* **44**, 354.

LEW, H. S. & FUNG, Y. C. 1969 *Biorheology*, **6**, 109.

LIGHTHILL, M. J. 1968 *J. Fluid Mech.* **34**, 113.

MOFFATT, H. K. 1964 *J. Fluid Mech.* **18**, 1.

NEWTON, R., REDBERGER, P. J. & ROUND, G. F. 1964 *Can. J. Chem. Eng.* **42**, 168.

RAYLEIGH, LORD 1920 *Scientific Papers*, vol. 6, p. 18. Cambridge University Press.

RUNCHAL, A. K. & WOLFSHTEIN, M. 1969 *J. Mech. Eng. Sci.* **11**, 445.

VARDY, A. E. 1971 Ph.D. thesis, University of Leeds.

WANG, H. & SHALAK, R. 1969 *J. Fluid Mech.* **38**, 75.

WEISS, R. F. & FLORSHEIM, B. H. 1965 *Phys. Fluids*, **8**, 1631.